Short communication

Nano-sponge ionic liquid–polymer composite electrolytes for solid-state lithium power sources

Kang-Shyang Liao [a,*], Thomas E. Sutto [b], Enrico Andreoli [a], Pulickel Ajayan [c], Karen A. McGrady [d], Seamus A. Curran [a]

[a] *Department of Physics, University of Houston, Houston, TX 77004, USA*
[b] *Naval Research Labs-DC, Materials Science and Technology Division, Washington, DC 20375, USA*
[c] *Department of Materials Engineering, Rice University, Houston, TX 77005, USA*
[d] *Marine Corps System Command, 50 Tech Parkway, Garrisonville, VA 22463, USA*

ARTICLE INFO

ABSTRACT

Solid polymer gel electrolytes composed of 75 wt.% of the ionic liquid, 1-*n*-butyl-2,3-dimethylimidazolium bis-trifluoromethanesulfonylimide with 1.0 M lithium bis-trifluoromethanesulfonylimide and 25 wt.% poly(vinylidenedifluoro-hexafluoropropene) are characterized as the electrolyte/separator in solid-state lithium batteries. The ionic conductivity of these gels ranges from 1.5 to 2.0 mS cm^{-1}, which is several orders of magnitude more conductive than any of the more commonly used solid polymers, and comparable to the best solid gel electrolytes currently used in industry. TGA indicates that these polymer gel electrolytes are thermally stable to over 280 °C, and do not begin to thermally decompose until over 300 °C; exhibiting a significant advancement in the safety of lithium batteries. Atomic force microscopy images of these solid thin films indicate that these polymer gel electrolytes have the structure of nano-sponges, with a sub-micron pore size. For these thin film batteries, 150 charge–discharge cycles are run for Li_xCoO_2 where x is cycled between 0.95 down to 0.55. Minimal internal resistance effects are observed over the charging cycles, indicating the high ionic conductivity of the ionic liquid solid polymer gel electrolyte. The overall cell efficiency is approximately 98%, and no significant loss in battery efficiency is observed over the 150 cycles.

1. Introduction

Current energy costs are becoming excessively prohibitive for sustained economic growth, an issue that will continue and become even more exacerbated in the next decade. The need to find an alternative in power generation that is both cheaper and sustainable pushes the interest in the alternative energy arena [1], although the potential problems have also been well reported and discussed in the past [2]. The world market for energy products is greater than $5 trillion dollars and growing with the demands of new emerging industrial markets. While significant interest is focused on generating alternative energy sources through the use of wind or solar, particular attention is also focused on how this energy can be stored [3–5]. Generation is only one side of a complex but fundamentally important technological problem. Increasing resources are being invested in the field of nanotechnology, in particular when focusing on energy and developing the next generation of nanomaterials for energy and nanoelectronic devices [6]. In particular, carbon based advances through the creation of engineered nanomaterials and engineered nanoscale interfaces have opened up the potential use of more lightweight and nano-defined technologies [7–9]. Combining polymers as a host in nanocomposites and hybrids has gained significant attention, and this has been found to be of particular interest in energy technologies [10–13].

As storage becomes more important in alternative technologies, these systems are evolving the need for safe, compact, rechargeable power sources continues to grow. Lithium ion batteries, the system of choice, use electrolytes which are volatile and flammable, leading to a number of safety concerns, which severely limit their overall usefulness [14]. Current industrial attempts to improve the safety of these electrolytes have focused on creating solid-state batteries using polymer or ceramic/glass solid electrolytes [15–17]. However, these materials have very poor ionic conductivities (<10^{-5} and <10^{-2} mS cm^{-1}, respectively), which limits their viability by significantly limiting the amount of current that can be drawn from a battery. Adding organic electrolytes as plasticizers to the polymers results in improved conductivities, but reintroduces the problems of volatility and flammability.

* Corresponding author at: Department of Physics, 617 Science & Research Building 1, University of Houston, Houston, TX 77004, USA. Tel.: +1 713 743 3565; fax: +1 713 743 3589.
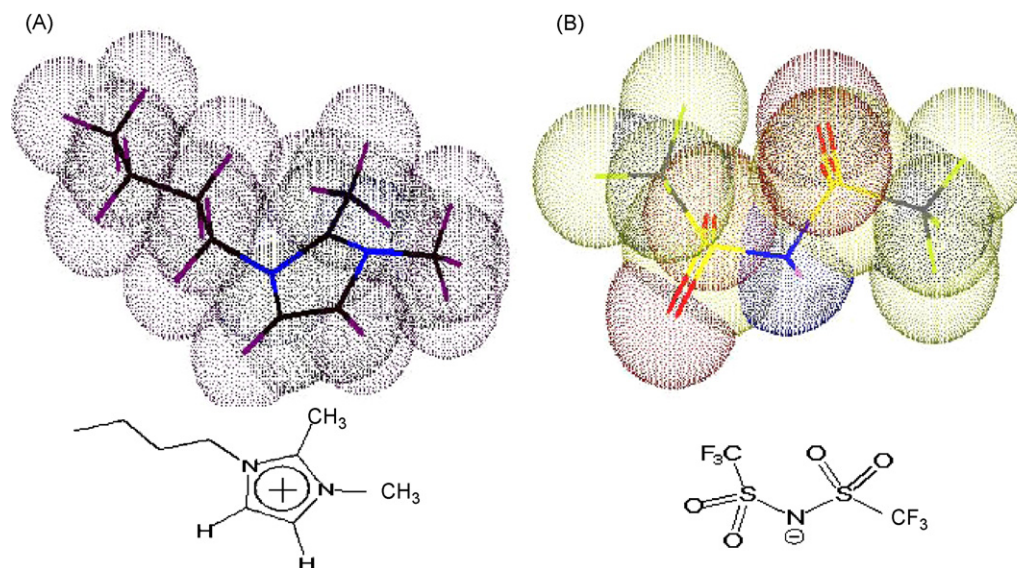*E-mail address:* kliao@mail.uh.edu (K.-S. Liao).

Fig. 1. VDW dot structure of (A) 1-*n*-butyl-2,3-dimethylimidazolium cation and (B) bis-trifluoromethanesulfonylimide anion.

There is an exponential growth rate in research publications where ionic liquids, organic-based molten salts that are liquid at ambient temperatures, figure prominently [5,18–23]. In general, the composition of these ionic liquids incorporates an asymmetrically substituted ring system with a positive charge, and numerous types of anions such as the halides or various fluorinated anionic species. The development of ionic liquids that use asymmetric substitutions of the five-membered imidazolium ring has enhanced their thermal and electrochemical stability significantly in the past decade, leading to their use as solvents for general organic syntheses and industry based polymer preparation [5,18]. It is this stability, owing both to their classification as a salt as well as the stability of the organic components that has made them attractive alternatives to the more common organic solvents. As salts, ionic liquids have almost no vapor pressure and as such are non-volatile. The presence of both positively and negatively charged species also tend to give them high values of ionic conductivity. Additionally, their dual salt and organic nature tend to make them useful as universal solvents. All of these factors combine to make them the ideal replacement for the more common, volatile electrolytes used in today's state-of-the-art Li-ion batteries.

Previous attempts to incorporate ionic liquids into lithium batteries indicated that after only 50 cycles, the efficiency and capacity of the battery significantly decreased [24]. This was due to either the instability of the di-substituted imidazolium cation, which is the more common cation chosen for ionic liquids, or due to degradation of the cathodes and anodes due to their interactions with the anions chosen. Additionally, the more commonly chosen anion, the tetrachloroaluminate anion ($AlCl_4^-$) is extremely moisture sensitive. This will evolve both heat and hydrochloric gas upon exposure to atmospheric moisture, thus eliminating the potential safety advantages of ionic liquids. The ionic liquid chosen for this work, 1-*n*-butyl-2,3-dimethylimidazolium bis-trifluoromethanesulfonylimide, $BMMI^+$ $TFSI^-$ (Fig. 1), overcomes these drawbacks by having a methyl group substituted at the 2-position on the imidazolium ring, which significantly enhances its electrochemical and thermal stability [18]. Secondly, the anion chosen, bis-trifluoromethanesulfonylimide ($TFSI^-$) anion, has already been shown to be electrochemically stable in lithium ion batteries [11,14,18]. It forms an air stable, hydrophobic ionic liquid when coupled with the BMMI cation, thus allowing preparation of solid polymer gel electrolytes in air without degradation of the electrolyte.
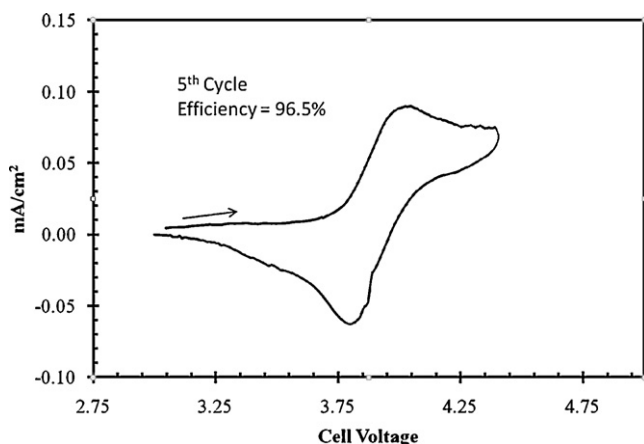
2. Experimental section

The ionic liquid used in this work, $BMMI^+$ $TFSI^-$ was prepared as described in literature [18]. For the purposes of lithium work, a 1.0 M solution using the lithium salt, lithium bis-trifluoromethanesulfonylimide (LiTFSI) was prepared (1.0 M Li/$BMMI^+$ $TFSI^-$). The charge–discharge capacity of a Li-battery using a $LiCoO_2$ cathode was characterized using metallic lithium as the anode, and a solid polymer gel composite electrode composed of 75 wt.% 1.0 M Li/$BMMI^+$ $TFSI^-$ and 25 wt.% poly(vinylidenedifluoro-hexafluoropropene) (PVDF-HFP). The polymer gel itself was prepared in a manner similar to that previously reported, except that acetone was used as the solvent to dissolve the ionic liquid and the polymer together because it allows for quick drying of the polymer gels.

Ionic conductivity of the polymer gel was measured on a Solartron 1260 Impedance Analyzer in stand-alone mode using a standard 2-electrode t-cell configuration. Thermogravimetric analysis of the solid polymer gel composite was carried out on a TA

Fig. 2. Cyclic voltammetry of the 5th cycling of a $LiCoO_2$ working electrode. The scan rate was 1 mV s^{-1}. The reference and counter electrodes were rods of Lithium metal.

Instruments TGA SDT 2960. 15 mg of the composite was placed in a sintered alumina crucible, the ramp rate was $5\,°C\,min^{-1}$ and the N_2 gas flow rate was $10\,cc\,min^{-1}$. Atomic force microscopy (AFM) images were collected using a Digital Instruments IIIa AFM in Tapping Mode to avoid problems associated with friction or tip adhesion to the soft composite surface. The AFM image shown corresponds to a scan area of $1.762\,\mu m \times 1.762\,\mu m$.

The battery assembly utilized $LiCoO_2$ cathodes prepared by blending the powder into a polymer composite solution composed of 87 wt.% $LiCoO_2$ (Aldrich, 99.95%), 3 wt.% graphite (Aldrich 99.999%, 1 μm size) and 10 wt.% PVDF-HFP dissolved in acetone. Discs of the Pt gauze (0.5 cm in diameter) were dip coated with this solution. Typically, 1 mg of material was deposited, or 0.8 (± 0.05) mg of $LiCoO_2$. The Li-metal anodes were 0.5 cm discs cut from high purity Li ribbon. Sandwiching a 0.5 cm disk of the polymer gel electrolyte (typically 1–2 mm thick) between an anode disk (the Li-metal disk) and a cathode disk (the $LiCoO_2$-polymer coated disk), and placing the stack between two Pt foil current collectors assembled the battery. These batteries were then charged for a total of 200 cycles at a capacity of $120\,mAh\,g^{-1}$ at a charging and discharging current of C/3, which was a surface area charging rate of approximately $40\,\mu A\,cm^{-2}$. All battery-charging experiments were performed in an Ar filled glove box (<1.0 ppm water and oxygen) using a PAR 273 potentiostat.

3. Results and discussion

The ionic conductivity was determined as the point at high frequency where the imaginary resistance component fell to zero. Measurements indicated that the ionic conductivity of the polymer gel was typically 1.5 up to $2.0\,mS\,cm^{-1}$ at room temperature. Temperature dependent measurements between $0\,°C$ and $120\,°C$ indicated typical deviations from classical Arrhenius behavior at the high ($11.1\,mS\,cm^{-1}$) and low ($1.05\,mS\,cm^{-1}$) temperature range. The macroscopic sponge-like behavior could be observed during these measurements since over-compression of the polymer gel resulted in a slight seeping out of the ionic liquid, which was re-absorbed when the pressure was removed.

Fig. 2 shows the cyclic voltammogram of the $LiCoO_2$ polymer composite electrode in the 1.0 M Li/BMMI$^+$ TFSI$^-$ electrolyte using the three-electrode cell. The 5th cycle is shown. The separation between the intercalation and deintercalation peak 0.40 mV, indicating that cycling improved the behavior of the electrode material. The overall efficiency was over 97%. The presence of the imida-
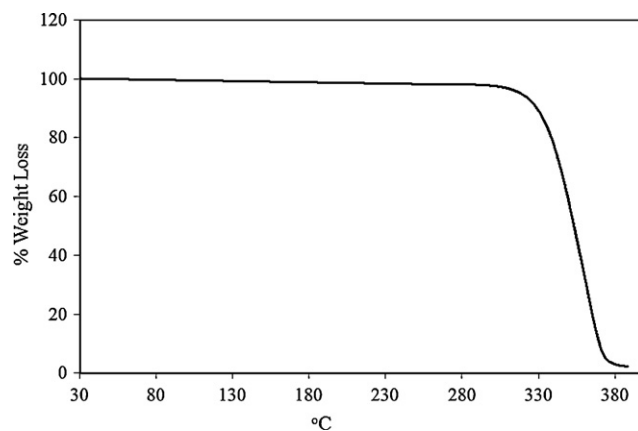

Fig. 3. Thermogravimetric analysis for 1-butyl-2,3-dimethylimidazolium bis-trifluoromethanesulfonylimide. Results are actual mass loss from the initial 15 mg sample of the polymer–ionic liquid nano-sponge.

zolium electrolyte did not cause significant degradation at the $LiCoO_2$ solid–electrolyte interface (SEI), which would otherwise hinder the kinetics of the intercalation and deintercalation causing the peak separation to increase. This also noticeably indicates the need for multiple initial cycles in order to obtain optimum performance of these power sources.

The stability of BMMI$^+$ TFSI$^-$ was tested by thermogravimetric analysis. As shown in Fig. 3, no weight loss was observed either by decomposition or volatilization of the ionic liquid until over $310\,°C$. This is over $200\,°C$ above the flash point of most common organic electrolytes.

The AFM and TEM images of the solid polymer–ionic liquid gel electrolyte were shown in Figs. 4 and 5, respectively. The crater-like features in the surface are considered to be pore openings, from 10 to 250 nm in diameter. Since previous work on the conductivity of ionic liquid polymer gel composites has shown that below a certain threshold wt.% of ionic liquid (approximately 65%) the ionic conductivity rapidly begins to decrease [5]. This, coupled with both the macroscopic and microscopic sponge-like qualities of the ionic liquid polymer gel composites studied here indicates that the ionic liquid is soluble in the polymer matrix to a certain point, but beyond that composition, the liquid component percolates out to form a nano-sponge, with multiple sub-micron channels of high ionic conductivity, resulting the formation of these extremely suit-
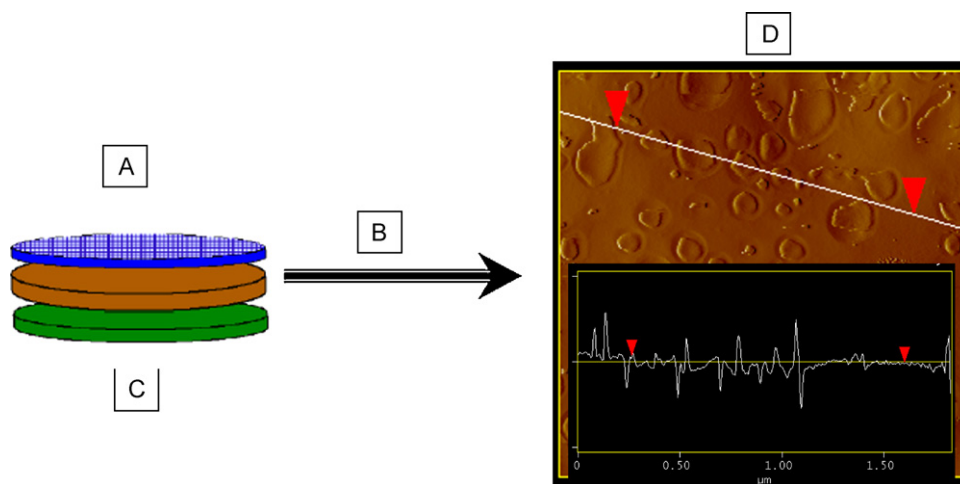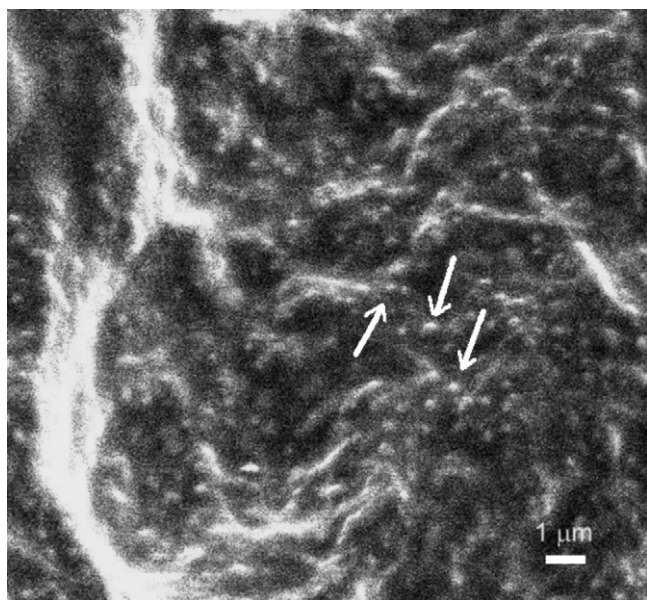

**Fig. 4.** Schematic cartoon of the solid-state lithium battery. (A) Pt gauze mesh coated with the 80% $LiCoO_2$ (cathode), (B) the solid polymer-ionic liquid nano-sponge gel electrolyte/separator, (C) the disk of lithium metal. (D) The AFM image of the solid polymer–ionic liquid gel electrolyte clearly showing the cratered surface with pore sizes in the 5–250 nm size range.

Fig. 5. TEM image of the solid polymer–ionic liquid gel electrolyte. The crater-like features (white arrows) in the surface are considered to be pore openings.

able polymer gel composite separators for lithium batteries. The stability and significance of the ionic liquid is due to the localized environment it is stored in. Mass storage of the liquid in a bulk environment allows destabilization of the liquid, however separating it out minimizes this process. The polymer acts as both storage and stabilizing host. It also means that within such an environment handling and managing the battery is far easier and more practicable.

The battery assembly utilized $LiCoO_2$ cathodes, solid polymer–ionic liquid nano-sponge gel electrolyte/separator and lithium metal was illustrated in Fig. 4. These batteries were then charged for a total of 200 cycles at a capacity of 120 mAh g^{-1} at a charging and discharging current of C/3, which was a surface area charging rate of approximately 40 μA cm^{-2}. The 200th charge–discharge cycle shown in the inset of Fig. 6 clearly indicates little IR drop in the cell at a discharge rate of C/3 using a Li-metal anode. Although the theoretical capacity of such a battery is near 135 mAh g^{-1}, the capacity was set lower than that since charging and discharging to higher capacities often results in voltage fade due to problems inherent with this material. Additionally, higher
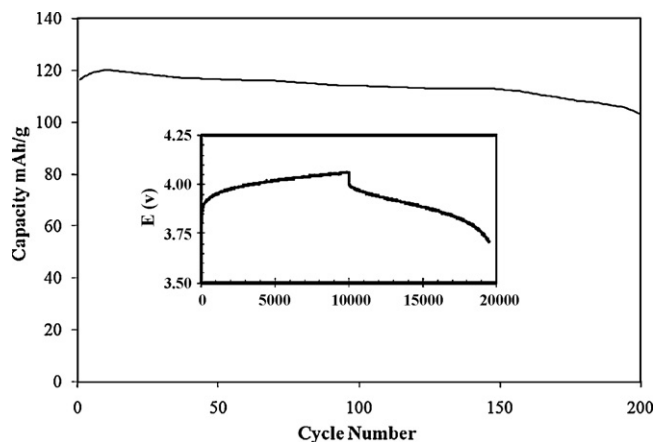
charge–discharge rates would be possible if thinner solid gel polymer electrolyte/separators were prepared, such as by spin coating. However, considering the environment we have stored the ionic liquid, we can see that the values already exhibited are a significant advance and are close to the limits of these ions. Most importantly, the percent efficiency clearly reaches a plateau near 98% within the first 5 cycles, and varies negligibly over the 200 cycles run. This closely parallels the ideal behavior seen in most of the current state-of-the-art battery work, except that these batteries are the first to incorporate a non-flammable ionic liquid, thus eliminating the dangers inherent in using flammable, volatile electrolytes.

Crucial to assessing the use of ionic liquids in Li-ion batteries is the reaction between metallic lithium and the ionic liquid. Previous work has shown that the tri-substituted imidazolium used here demonstrates significant electrochemical stability. However, one critical issue that must be addressed is the mobility of the cation and anion in the polymer gel. Recent work has shown that the mobility of the cationic and anionic components of these ionic liquids can readily intercalate and deintercalate graphite [25]. Originally, the cathode incorporated 10 wt.% graphite, which proved problematic in terms of overall capacity during cycling. Observations clearly showed a loss of capacity as the intercalation and dintercalation of the graphite in the cathode eroded it over time. However, by reducing the amount of graphite to only 3 wt.%, this problem was able to be eliminated. Future work will focus on using polymerized ionic liquids, in which the imidazolium cations are linked together to form a positively charged polymer backbone.

4. Conclusion

Previous work by numerous authors has shown that non-flammable ionic liquids are suitable replacements for many of the niches currently filled by volatile organic solvents. The nano-sponge separators are typically over 100 times more ionically conductive than ceramics or glasses, and over 10,000 times more ionically conductive than most solid polymers. They also possess a thermal decomposition point over 200 °C higher than common electrolytes, which is primarily due to the synthetic environment we have developed. Additionally, since the ionic liquid here has proven itself electrochemically stable enough for the high voltages reached in a lithium battery, and so consequently a lightweight stable step closer to more convenient and compact storage systems desired. We see from our work that it is very desirable to incorporate these types of polymer–ionic liquid nano-sponge gel electrolytes in place of the polymers, ceramics or glasses currently being studied. The results show that we have developed a system much more efficient, safe and robust that current state-of-the-art, improvements across all facets of battery materials currently studied or in operation. Incorporation of ionic liquids in place of the more volatile and flammable organic carbonate-based electrolytes in liquid lithium batteries is the next milestone in the advancement of widespread usage of ionic liquids in high energy density power sources.

Fig. 6. Effective Capacity over 200 cycles for the solid-state lithium battery using the solid polymer–ionic liquid nano-sponge electrolyte/separator. Inset is of the 200th charge–discharge cycle (C3 charge and discharge currents).

References

[1] M. Armand, J.M. Tarascon, Nature 451 (2008) 652–657.
[2] C.J. Cleveland, R. Costanza, C.A.S. Hall, R. Kaufmann, Science 225 (1984) 890–897.
[3] S. Roth, S. Blumentritt, M. Burghard, E. Cammi, D. Carroll, S. Curran, G. Dusberg, K. Liu, J. Muster, G. Philipp, T. Rabenau, Synth. Met. 94 (1998) 105–110.
[4] M. Reyes-Reyes, K. Kim, J. Dewald, R. Lopez-Sandoval, A. Avadhanula, S. Curran, D.L. Carroll, Org. Lett. 7 (2005) 5749–5752.
[5] T.E. Sutto, J. Electrochem. Soc. 154 (2007) P130–P135.
[6] D. Zhang, M.A. Kandadai, J. Cech, S. Roth, S.A. Curran, J. Phys. Chem. B 110 (2006) 12910–12915.

[7] A.B. Dalton, H.J. Byrne, J.N. Coleman, S. Curran, A.P. Davey, B. McCarthy, W. Blau, Synth. Met. 102 (1999) 1176–1177.

[8] J.M. Tarascon, M. Armand, Nature 414 (2001) 359–367.

[9] S.A. Curran, A.V. Ellis, A. Vijayaraghavan, P.M. Ajayan, J. Chem. Phys. 120 (2004) 4886–4889.

[10] D.L. Carroll, P. Redlich, P.M. Ajayan, S. Curran, S. Roth, M. Ruhle, Carbon 36 (1998) 753–756.

[11] F. Lemaitre-Auger, J. Prud'homme, Electrochim. Acta 46 (2001) 1359–1367.

[12] S.A. Curran, D. Zhang, W.T. Wondmagegn, A.V. Ellis, J. Cech, S. Roth, D.L. Carroll, J. Mater. Res. 21 (2006) 1071–1077.

[13] C. Combelles, M.L. Doublet, Ionics 14 (2008) 279–283.

[14] K. Hayamizu, Y. Aihara, S. Arai, Garcia, J. Phys. Chem. B 103 (1999) 519–524.

[15] O. Bohnke, C. Rousselot, P.A. Gillet, C. Truche, J. Electrochem. Soc. 139 (1992) 1862–1865.

[16] G. Nagasubramanian, L. Bronstein, J. Carini, J. Power Sources 162 (2006) 847–850.

[17] M.-S. Park, S.-H. Hyun, S.-C. Nam, S.B. Cho, Electrochim. Acta 53 (2008) 5523–5527.

[18] F.F.C. Bazito, Y. Kawano, R.M. Torresi, Electrochim. Acta 52 (2007) 6427–6437.

[19] M. Egashira, H. Todo, N. Yoshimoto, M. Morita, J. Power Sources 178 (2008) 729–735.

[20] A. Guerfi, S. Duchesne, Y. Kobayashi, A. Vijh, K. Zaghib, J. Power Sources 175 (2008) 866–873.

[21] A. Guerfi, M. Dontigny, Y. Kobayashi, A. Vijh, K. Zaghib, J. Solid State Electrochem. 13 (2009) 1003–1014.

[22] C. Sirisopanaporn, A. Fernicola, B. Scrosati, J. Power Sources 186 (2009) 490–495.

[23] T. Sugimoto, Y. Atsumi, M. Kikuta, E. Ishiko, M. Kono, M. Ishikawa, J. Power Sources 189 (2009) 802–805.

[24] K. Dahl, G.M. Sando, D.M. Fox, T.E. Sutto, J.C. Owrutsky, J. Chem. Phys. 123 (2005) 084504–084511.

[25] T.E. Sutto, T.T. Duncan, T.C. Wong, Electrochim. Acta 54 (24) (2009) 5648–5655.